

Production of argon isotopes by spallation of Sc, Ti, Fe, Co, Ni, and Cu

S. Regnier

Centre d'Etudes Nucléaires de Bordeaux-Gradignan, Laboratoire de Chimie Nucléaire, E.R.A. n° 144, Le Haut Vigneau-33170-Gradignan, France

(Received 20 February 1979)

Spallation ratios and production cross sections of $^{36,38,39,42}\text{Ar}$ have been measured for the interaction of 0.080, 0.150, 0.600, 1.05, and 24 GeV protons with scandium, titanium, iron, cobalt, nickel, and copper. Argon is measured by means of a 60° 12 cm radius mass spectrometer, equipped with a gas extraction line and a calibration system. Precision is 1 to 5% for isotope ratios, and 10 to 20% for the cross sections. With regard to spallation reactions, some systematic effects are shown or confirmed. Excitation functions go through a maximum at high energy, then drop asymptotically to a constant value. The ratio of maximum to asymptote cross sections is about 1.6. The spallation ratios depend linearly on the $(N/Z)_T$ ratios of the target and there is probably a linear correlation between the position of the peak of the spallation distribution and the $(N/Z)_T$ ratio. Experimental values are compared with semiempirical fits and some astrophysical implications are discussed.

NUCLEAR REACTIONS Spallation; targets Sc, Ti, Fe, Co, Ni, Cu; protons 0.080, 0.150, 0.600, 1.05, 24 GeV; measured σ for formation of $^{36, 38, 39, 42}\text{Ar}$; mass spectrometry; σ compared with semiempirical calculations; astrophysical implications.

I. INTRODUCTION

Spallation of the elements of medium mass has been the subject of numerous experimental studies. For the most part, these concerned the radioactive reaction products (see, for example, Refs. 1 to 10 and the compilations of Brunix,¹¹ Silberberg *et al.*,¹² and Tobailem *et al.*¹³), whereas the stable products, although accounting for a considerable part of the inelastic cross section, have been the subject of a limited number of studies (Schaeffer *et al.*,¹⁴ Hudis *et al.*,¹⁵ Husain *et al.*,¹⁶ and Perron¹⁷).

The general characteristics of the spallation of medium-mass targets are well reproduced by the two-step model of Serber.¹⁸ Because of the great complexity of the "particle + nucleus" interactions in the GeV energy range, however, the mathematical developments of the model have all failed to predict precise cross sections for incident energies considerably beyond the threshold for meson production. For this reason, since the original work of Rudstam,^{19,20} much effort has been devoted to the prediction of cross sections by means of semiempirical formulas, where the cross section $\sigma(A, Z)$ for a product (A, Z) and a target (A_T) is given by

$$\sigma(A, Z) = \sigma_0(A_T) e^{-P\Delta A} G(A, Z) \dots, \quad (1)$$

where $\sigma_0(A_T)$ is related to the inelastic cross section of the target; $e^{-P\Delta A}$ includes the excitation functions and describes the experimental decrease of the cross sections when $\Delta A (= A_T - A)$ increases;

$G(A, Z)$ is a Gaussian or quasi-Gaussian function describing the charge distribution of the spallation products. Depending on the particular formulations of Eq. (1), other factors which vary with the energy and the nature of products or target are also included.

A knowledge of spallation cross sections, particularly for medium-mass targets, is indispensable for the understanding of the interactions of galactic cosmic rays (GCR) with the interstellar medium and extraterrestrial materials. The interpretation of these interactions provides information on the history of the solar system and on the sources and propagation of the GCR. (For details, see reviews by Reeves,²¹ and Shapiro *et al.*²² or Reedy and Arnold.²³) Cross sections for all the nuclear reactions which can occur are required as input parameters for models describing cosmic ray interaction with the interstellar medium or with meteorites or the lunar surface. The semiempirical formula most frequently employed at the present time is that of Silberberg and Tsao,²⁴ which gives considerable precision over the widest range of targets and products. The definition of the parameters of the semiempirical formula (i.e., the prediction of unknown σ) can evidently be improved by a coherent body of experimental cross sections obtained under well-defined conditions.

Although the general characteristics of spallation reactions are now well known, certain aspects are not yet entirely clear. Two of these are the subject of the present study.

(a) How important is the influence of target com-

position on the final distribution of spallation products, in the case of medium-mass targets? For heavier targets, such influence was observed by Porile and Church²⁵ in their study of the isobars of mass 72 produced by 1.8 GeV protons interacting with ⁹⁶Zr, ⁹⁶Mo, and ⁹⁶Ru, and by Ku and Karol²⁶ in their recent study of the same isobars produced by 720 MeV α particles interacting with ⁹²Mo, ⁹⁶Mo, and ¹⁰⁰Mo. According to these authors, the distribution of spallation products depends on the ratio (N/Z) of the target nucleus.

(b) The excitation functions for spallation reactions increase rapidly between the reaction threshold and about 1 GeV, then tend towards an asymptotic value, with no significant variation being observed above about 10 GeV. It is yet to be determined, however, whether the cross sections go through a maximum somewhere in the 1–10 GeV interval.

The present article describes the measurement of the cross sections for four isotopes of argon, two stable (36, 38) and two of long period (39, 42), produced by proton bombardment of six medium-mass targets (Sc, Ti, Fe, Co, Ni, and Cu). Five proton energies were employed; 0.08, 0.15, 0.6, 1.05, and 24 GeV. The results are used to obtain excitation functions and mass-distribution curves. The influence of target structure on mass distribution is discussed, using the present results and those already published for similar target and product ranges. The existence of a maximum for the excitation functions is inferred if the cross sections at 1 GeV is greater than at 24 GeV.

II. EXPERIMENTAL METHODS

The targets consisted of stacks of 20×20 mm squares of metal foil of thickness 0.010 to 0.050 mm. Al foil was inserted between the target foils (Sc, Ti, V, Fe, Co, Ni, and Cu) to serve as guards, recoil collectors, and monitors. The thicknesses of the stacks were 0.15 g/cm² for the irradiation at 0.080 GeV, 0.3 to 0.5 g/cm² at 0.15, 0.6, and 24 GeV, and 1.5 g/cm² at 1.05 GeV. Each target contained either 3 or 6 monitors. All the results for the vanadium targets were lost due to experimental problems.

The irradiations were carried out in the following accelerators: Louvain-la-Neuve (0.080 GeV), Saturne (1.05 GeV), Orsay (0.150 GeV), and CERN (0.6 and 24 GeV). In most cases, the internal beam and the maximum intensity were used. However, three irradiations with the CERN external beam and one low intensity irradiation at Louvain were used to test the influence of beam intensity on the loss of argon due to heating. No intensity dependence was observed.

The total proton flux through a target was calculated by means of the monitor reaction, ²⁷Al($p, 3p3n$)²²Na, for which the cross sections²⁷ are 22.7, 17.2, 17.3, 15.3, and 10 mb, respectively, at 0.080, 0.150, 0.600, 1.05, and 24 GeV. The integrated flux employed varied from 0.5 to 5 × 10¹⁷ protons. It was ascertained from the monitor measurements that the targets were properly aligned and that the flux was homogeneous within the stack to better than 5% (1 to 5%). In general, each target element was subjected to three independent irradiations at each energy E_p , and two years, at least, elapsed between irradiation and analysis. The effect of secondary particles must be considered only for targets having a small ΔA with the spallation products.⁶ The good agreement between the different monitors within each particular target stack indicates rather small contributions from secondaries in the present experiments. Also, the position of each target element varied during the independent irradiations at one particular energy. No systematic trend was observed and the effect of secondary particles is believed to be accounted for in the error bars associated with the results given below.

The techniques employed for the measurement of the argon produced by spallation have been described elsewhere.²⁸ The argon is extracted in an off-line system, by melting of the target under vacuum in a molybdenum crucible, heated by induction (1200°–1800 °C, depending on the metal). The extracted gas was purified by means of two titanium getters (successively cooled from 700° to 200 °C) then adsorbed on activated charcoal at –196 °C in a glass tube which could be sealed off for subsequent analysis. Second extractions and blank runs were frequently carried out. The argon samples were analyzed in a 60° sector, 12 cm radius mass spectrometer (a modified MICRO-MASS 12) with which accurate isotope ratios could be obtained with only 10⁷ to 10¹¹ atoms of each species, thanks to the small internal volume of the instrument and its excellent behavior under static vacuum conditions.

The mass spectrometer was calibrated by introducing precisely measured quantities of air, prepared in an independent system composed of several known expansion volumes and a capacitance manometer.

The isotope ratios were subjected to several corrections, the most important of which was due to the presence of atmospheric argon in the target metals (which also prevented the measurement of ⁴⁰Ar produced by spallation). It was assumed that all ⁴⁰Ar was atmospheric, except a small part deduced in an iterative procedure from the charge-dispersion curves. Hydrocarbon ions were always

TABLE I. Argon isotope ratios and cross sections (in mb) for the targets Sc, Ti, V, Fe, Co, Ni and Cu as functions of the incident energy E_p (in GeV). Where necessary, values from other publications have been corrected for the monitor cross section.

E_p (GeV)	38/36	38/39	38/42	^{36}Ar	^{38}Ar	^{39}Ar	^{42}Ar	Ref.
0.080	Sc	25.2 \pm 1.8	2.77 \pm 0.04	1.43 \pm 0.16	35.9 \pm 3.2	13.0 \pm 1.0		
	Sc	10.0 \pm 0.5	2.33 \pm 0.03	2.85 \pm 0.37	28.5 \pm 3.4	12.2 \pm 1.5	0.034 \pm 0.014	
	Ti	12.40 \pm 0.15	1.86 \pm 0.02	1.15 \pm 0.17	14.2 \pm 2.1	7.6 \pm 1.1	0.095 \pm 0.014	
0.150	Fe		1.91 \pm 0.07		0.34 \pm 0.02	0.18 \pm 0.02		
	Co	16.5 \pm 0.9	1.39 \pm 0.03	0.0035 \pm 0.006	0.058 \pm 0.009	0.042 \pm 0.007	0.0007 \pm 0.00015	
	Ni	5.9 \pm 0.4	2.75 \pm 0.06	0.014 \pm 0.003	0.080 \pm 0.015	0.029 \pm 0.006	0.0006 \pm 0.0003	
0.150	Fe					0.25 \pm 0.02		30
0.600	Fe	8.31 \pm 0.28	2.02 \pm 0.02	1.49 \pm 0.17	12.4 \pm 1.3	6.1 \pm 0.7	0.050 \pm 0.015	
	Cu	11.33 \pm 0.16	1.67 \pm 0.02	0.38 \pm 0.02	4.3 \pm 0.2	2.6 \pm 0.1	0.057 \pm 0.003	
0.600	Fe			1.13 \pm 0.12	9.8 \pm 1.0	5.1 \pm 0.5		29
	Cu			0.46 \pm 0.05	5.1 \pm 0.5	2.9 \pm 0.3	0.060 \pm 0.006	29
1.0	Ni					5.5 \pm 0.6		30
	Sc	9.6 \pm 1.0	2.03 \pm 0.04	2.9 \pm 0.4	27.8 \pm 2.1	13.7 \pm 1.1	0.11 \pm 0.02	
	Ti	9.0 \pm 0.2	1.81 \pm 0.04	3.4 \pm 0.3	30.6 \pm 2.9	16.9 \pm 1.6	0.49 \pm 0.05	
1.05	Fe	7.3 \pm 0.5	2.02 \pm 0.03	2.5 \pm 0.3	18.2 \pm 1.9	9.0 \pm 1.0	0.11 \pm 0.02	
	Co	9.6 \pm 0.2	1.78 \pm 0.03	1.8 \pm 0.3	16.9 \pm 2.5	9.5 \pm 1.4	0.20 \pm 0.03	
	Ni	5.37 \pm 0.10	2.37 \pm 0.04	2.6 \pm 0.2	14.1 \pm 1.0	6.0 \pm 0.4	0.048 \pm 0.005	
	Cu	9.9 \pm 0.4	1.75 \pm 0.07	1.00 \pm 0.17	10.0 \pm 1.6	5.7 \pm 0.9	0.14 \pm 0.03	
3.0	Fe					6.7 \pm 0.2	0.101 \pm 0.004	31
	Sc	9.5 \pm 0.9	1.92 \pm 0.09	1.75 \pm 0.23	16.6 \pm 1.5	8.7 \pm 0.9	0.090 \pm 0.012	
	Ti	9.4 \pm 0.2	1.73 \pm 0.02	1.93 \pm 0.14	18.1 \pm 1.3	10.4 \pm 0.8	0.38 \pm 0.03	
	Fe	7.2 \pm 0.2	1.98 \pm 0.02	1.37 \pm 0.18	9.8 \pm 1.3	5.0 \pm 0.7	0.084 \pm 0.012	
24.0	Co	9.00 \pm 0.13	1.79 \pm 0.02	1.30 \pm 0.14	11.7 \pm 1.3	6.5 \pm 0.7	0.22 \pm 0.06	
	Ni	5.05 \pm 0.08	2.37 \pm 0.03	2.09 \pm 0.15	10.6 \pm 0.7	4.5 \pm 0.3	0.046 \pm 0.004	
	Cu	9.00 \pm 0.08	1.760 \pm 0.015	1.06 \pm 0.14	9.5 \pm 1.2	5.4 \pm 0.7	0.15 \pm 0.02	
25.0	Fe			1.9 \pm 0.2	16.9 \pm 1.7	9.3 \pm 0.9		29
	Cu			1.14 \pm 0.11	10.9 \pm 1.1	6.2 \pm 0.6		29
28.0	Fe					6.0 \pm 0.6		30
	Ni					4.5 \pm 0.5		30
	Cu					5.5 \pm 0.7	0.17 \pm 0.02	6
29.0	V	11.6	1.53			10.3 \pm 1.0	0.54 \pm 0.11	16
	Fe			1.36 \pm 0.2	15.8 \pm 2.4	6.0 \pm 0.2	0.104 \pm 0.012	31
	Cu			1.22 \pm 0.10	11.3 \pm 1.0	6.5 \pm 0.5	0.16 \pm 0.03	15

negligible, except at mass 42 in the case of Sc and Fe targets. The other corrections were occasioned by discrimination and memory effects in the mass spectrometer. Second extraction at higher temperature always gave less than 1% of the total argon obtained from a given target.

III. RESULTS

Table I gives the argon isotope ratios 38/36, 38/39, and 38/42 and the cross sections for 36, 38, 39, and 42 for the targets studied here and elsewhere, as functions of the incident energy E_p . In general, each value is the average of three independent measurements. The cross sections for ^{38}Ar and ^{39}Ar are cumulative and those for ^{36}Ar and ^{42}Ar are independent. The uncertainties have been determined as follows. In the first place, the root mean square of the various errors is calculated for each measurement, i.e., target preparation (thickness, 0.5 to 3%; impurities, 0 to 1%), monitoring and alignment (3 to 7%), blanks for apparatus and metals (in most cases, 0 to 1%; sometimes 1 to 80%), zero-time corrections to mass-spectrometer analysis (0 to 1%; sometimes 1 to 5%), re-extractions (0 to 1%), and calibration (7 to 12%). For the isotope ratios the most important errors cancel out, but an error of 2% is added to account for a possible systematic instrumental error. Altogether, the uncertainty of a cross section measurement is generally from 10 to 20%, whereas that of the ratios is from 2 to 5%. The mean of the independent measurements x_i is then calculated, weighting each of these by the inverse of the square of its uncertainty, Δx_i . Thus, σ or R is given by

$$\sum_i (x_i/\Delta x_i^2) / \sum_i (1/\Delta x_i^2).$$

The uncertainty given in Table I is the standard deviation from the mean of the independent measurements, or the quantity

$$\Delta\sigma \text{ (or } \Delta R) = \left[\sum_i (1/\Delta x_i^2) \right]^{1/2},$$

whichever is the larger.

The present results may be compared (Table I) with those already published by others, mainly for argon isotopes in Fe and Cu. Where necessary, the cross sections have been corrected to correspond to the same monitor cross section. Agreement with the values of Goebel *et al.*²⁹ is good for Fe and Cu at 600 MeV and for Cu at 25 GeV, but rather bad for Fe at 25 GeV. Excellent agreement is found between the present values and those of Hudis *et al.*¹⁵ for Cu at 29 GeV, Foreman *et al.*³⁰ for ^{39}Ar in Fe and Ni at 0.15, 1.0, and 28 GeV, Cum-

ming *et al.*⁶ for Cu at 28 GeV and Cheng³¹ for ^{39}Ar and ^{42}Ar in Fe at 0.6 and 29 GeV. It may be noted that most of these authors estimated ^{39}Ar and ^{42}Ar by radioactivity measurements.

Table I also shows the value of Husain and Katcoff¹⁶ for V at 29 GeV. These values will be referred to in the following discussion.

IV. DISCUSSION

Three main questions will be discussed below: the dependence of cross sections on the incident energy E_p , the influence of the ratio N/Z of the target on the argon isotope distribution, and the validity of the semiempirical formula of Silberberg and Tsao²⁴ in the energy region studied. In addition, some astrophysical implications of the results will be mentioned.

A. Excitation functions

Excitation functions for the formation of argon isotopes can be constructed from the results in Table I. Some of these are shown in Figs. 1 to 5. When ΔA is about 20 or higher, as for Figs. 1 to 4, the cross sections increase by a factor of 10^3 between about 0.15 and 1 GeV. This corresponds to an increase of the probability of formation of very excited intermediate nuclei at the exit from the cascade step. At still higher energies, the excitation functions are observed to saturate and the cross sections appear to fall asymptotically by a factor of 1.5 to 2 towards a constant value. The probability of forming very excited intermediate nuclei must then no longer increase with the incident energy E_p . Most of the incident energy is

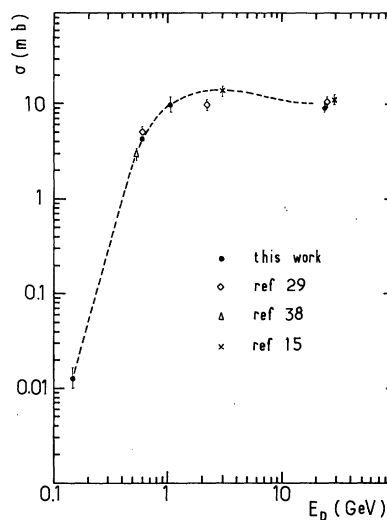


FIG. 1. Proton spallation cross sections for production of ^{38}Ar from copper. The dashed curve is the manual best fit.

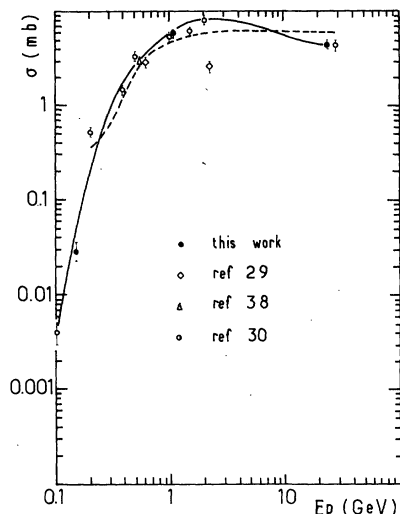


FIG. 2. Proton spallation cross sections for production of ^{39}Ar from nickel. The solid curve is the manual best fit. The dashed curve is calculated by ST (Ref. 24).

then recovered as kinetic energy or absorbed in the creation of particles. According to Barashenkov,³² the development of the intranuclear cascade lowers the nuclear density when E_p reaches several GeV, leading to saturation of the number of possible interactions during this first step and causing the excitation energy E^* to reach a limit. It has also been suggested that, in this energy region, multiple-particle interactions can play an important role in disposing of the excess incident energy. When ΔA is less than 10 nucleons, the variation

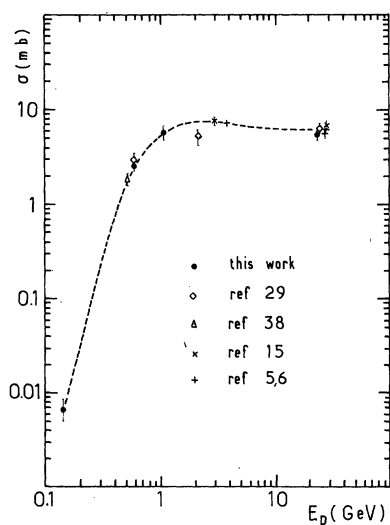


FIG. 3. Proton spallation cross sections for production of ^{39}Ar from copper. The dashed curve is the manual best fit.

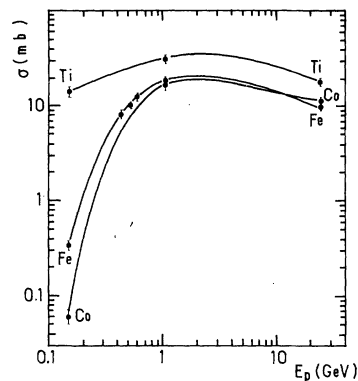


FIG. 4. Proton spallation cross sections for production of ^{38}Ar in titanium, iron, and cobalt.

of cross section with projectile kinetic energy is much smaller in the range 0.1 to 1 GeV, as may be seen in Fig. 5 for Ar isotope production in Sc [mainly $(p, 4pxn)$ reactions] and in Fig. 4 for ^{38}Ar in Ti.

In the case of spallation of nuclei of medium mass, it has been shown in this laboratory³³ that the mean excitation energy may be written E^* (in MeV) $\approx 8\Delta A$. The factor 8 corresponds to the binding energy per nucleon, which to a first approximation is independent of the mass of the nucleus. In the reactions studied here, ΔA varies from 3 to 28 nucleons, corresponding to $E^* \sim 25$ to 225 MeV. These values may appear small compared to incident energies of several GeV, but they are not

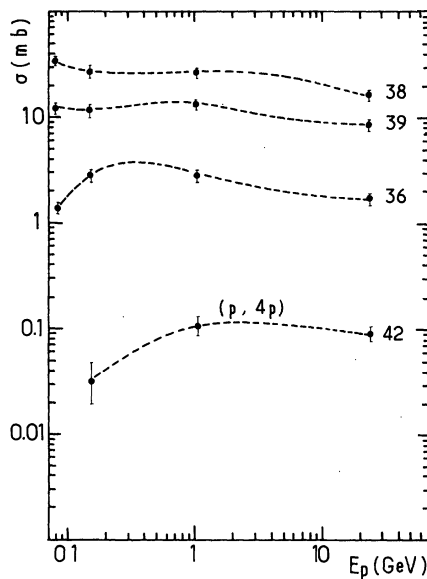


FIG. 5. Proton spallation cross sections for production of $^{38-42}\text{Ar}$ in scandium, mainly by $(p, 4pxn)$ reactions.

small compared to the total binding energies of the target nuclei, which range from 360 MeV for Sc to about 500 MeV for Cu.

Numerous excitation functions have already been published for targets of medium mass. Examination of some of these² suggests they might pass by a maximum before tending towards a horizontal asymptote. The existence of such maxima are clearly demonstrated by the results of the present study (see Figs. 1 to 6).

It can be seen from Table I that most of the cross sections fall appreciably between 1 and 24 GeV. Taking the argon isotopes 36, 38, and 39 and the targets Sc, Ti, Fe, Co, and Ni, the mean ratio of the 15 cross sections for 1 and 24 GeV is

$$(\sigma_1/\sigma_{24}) = 1.58 \pm 0.20.$$

Inspection of the excitation functions for these reactions (Figs. 1 to 5) suggests that the maximum is not reached at 1 GeV but rather at an incident energy of about 2 GeV for Ar in Cu and Ni and probably varies with ΔA for the other targets. Figure 6 shows the ratios σ_1/σ_{24} as a function of ΔA for all the reactions studied in the present work. The error bars indicate the mean squares of the uncertainties. For argon 36, 38, and 39, and $6 \leq \Delta A \leq 18$, all the ratios σ_1/σ_{24} are greater than 1.5. When ΔA falls between 20 and 23, $(\sigma_1/\sigma_{24}) > 1.3$ and for $\Delta A > 24$, $\sigma_1/\sigma_{24} \approx 1$. The ratio σ_1/σ_{24} thus tends to pass by a maximum as ΔA increases. The same tendency exists for ^{42}Ar , but the maximum is less pronounced.

It would evidently be interesting, particularly for the applications of spallation reactions, to know the ratios of the maximum to the asymptote for the excitation functions, and work in pursuit of that goal is in progress in this laboratory. Preliminary results, combined with those of Brodzinski *et al.*² and Raisbeck *et al.*,^{34,35} concern 19 reactions in which ΔA varies from 8 to 25 and the

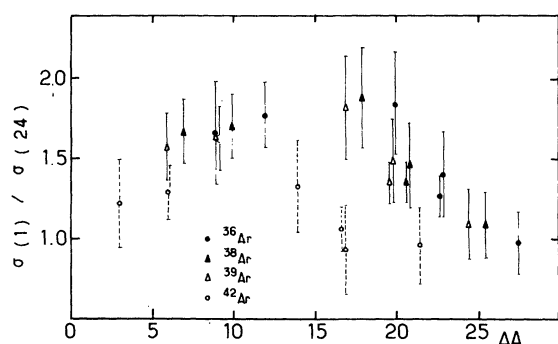


FIG. 6. Ratios for cross sections of Ar isotopes from medium mass targets bombarded with 1.05 and 24 GeV protons versus $\Delta A = A_T - A$.

energy at the maximum from about 0.5 to about 2 GeV. The cross section ratios (maximum/asymptote) obtained vary from 1.3 to 2, with a mean value of 1.63 ± 0.24 . This effect could contribute to the calculated variations of the mean free path of galactic cosmic rays in the GeV region.

In terms of the two-step model, the significance of the maximum is probably as follows: The cross section σ for a given reaction increases as long as the probability of formation of appropriately excited ($E^* \approx 8\Delta A$) cascade nuclei increases. When the incident energy exceeds the optimum value for that reaction, the mean excitation energy increases, favoring reactions with greater ΔA and lowering σ . Beyond about 10 GeV, the excitation energy spectrum becomes invariant³⁶ for all the reasons given above (and perhaps for others), and the cross sections become constant.

It should be noted that the above conclusions depend on the correctness of the monitor reaction cross sections. Owing to the rather long irradiation times, the $^{27}\text{Al}(p, 3p3n)^{22}\text{Na}$ reaction is preferred to the $^{27}\text{Al}(p, 3pn)^{24}\text{Na}$ reaction, for which the cross sections are more accurately known. The ratio of 1 to 24 GeV cross sections of the latter reaction is 1.24, and can be considered as a lower value for the $^{27}\text{Al}(p, 3p3n)^{22}\text{Na}$ reaction (a ratio of 1.53 was used in the present study). Therefore the magnitude of the effect shown in Fig. 6 cannot be explained by a systematic error in the monitor cross sections.

B. Influence of the ratio N/Z of the target

Examination of Table I shows two complementary effects. In Ni, the neutron-deficient isotope ^{36}Ar is markedly preferred and the neutron-rich isotope ^{42}Ar markedly suppressed, compared with the targets of neighboring atomic number, Co and Cu. In this respect, it may be noted that the ratio $(N/Z)_T$ for Ni is 1.100, whereas the ratios for Co and Cu are 1.185 and 1.194, respectively. Ni may thus be considered to be a "neutron-poor" target. The inverse effect is observed for ^{36}Ar and ^{42}Ar in V, for which the ratio $(N/Z)_T = 1.217$ is the largest of all, for the targets considered here. It would seem, therefore, that the apparent incoherence of the spallation ratios of argon, when the targets are arranged in the order of the atomic numbers, may be interpreted as a "memory effect" with regard to the target. For $E_p = 24$ GeV, Fig. 7 shows a strong correlation between the spallation ratios of argon measured here and the $(N/Z)_T$ ratios for Ti, V, Fe, Co, Ni, and Cu (Sc is excluded, ΔA being too small). The same correlation exists at all the energies E_p , as may be seen in Table II, which gives the slopes of the lin-

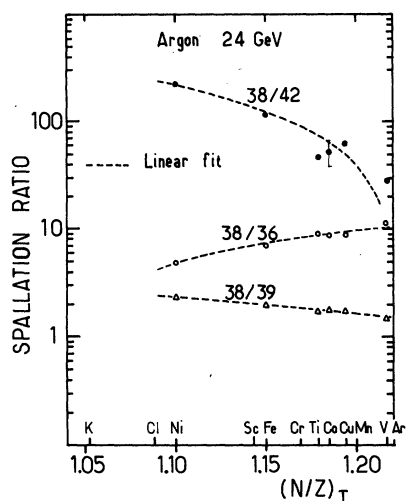


FIG. 7. Spallation ratios for Ar isotopes from medium mass targets bombarded with 24 GeV protons versus $(N/Z)_T$. The dashed lines are the linear fits (note the semilog scale).

ear fits for 0.15, 1.05, and 24 GeV. The same conclusion is reached with the ratios $^{42}\text{K}/^{43}\text{K}$ for $E_p = 0.6$ GeV, measured by Lagarde-Simonoff *et al.*³ and the ratios $^{22}\text{Na}/^{24}\text{Na}$ for $E_p = 0.4$ GeV given by Korteling *et al.*³⁷ The linear correlation between $(N/Z)_T$ and the spallation ratios deduced from the results of the above authors is clearly shown in Fig. 8. Table II shows the slopes of the corresponding linear fits.

A strong dependence of the spallation ratios on $(N/Z)_T$ has also been recently observed by Ku and Karol,²⁶ in a study of the isobars with $A = 72$ produced in the spallation of ^{92}Mo , ^{96}Mo , and ^{100}Mo , bombarded by 720 MeV α particles. The same effect had been observed by Porile and Church²⁵ with targets of ^{96}Ru , ^{96}Mo , and ^{96}Zn , bombarded by 1.8 GeV protons. With these results, in addition to those given in the present work, it may be considered that the target memory effect in spallation reactions is well established.

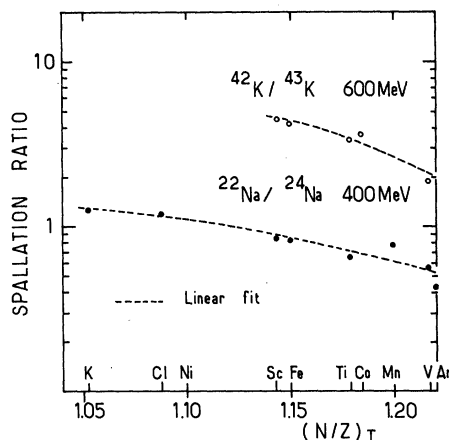


FIG. 8. Spallation ratios for K and Na isotopes from medium mass targets bombarded with 600 and 400 MeV protons versus $(N/Z)_T$. As in Fig. 7, a linear fit is observed. Data are from Refs. 3 and 37.

Generally, the distribution of spallation products in a given mass interval (here, $A = 36$ to 42) is shown by plotting the N/Z ratio of the product (abscissa) against the independent cross section (ordinate). The charge dispersion, or cd curves are constructed from the measured cross sections (often cumulative) by successive approximations, giving the independent cross sections after two or three iterations. A Gaussian or quasi-Gaussian form is imposed on the distributions, and the parameters of the fitting function are determined by least squares method. When a Gaussian form is imposed, it thereby becomes impossible to account for small cross sections and for asymmetrical distributions. However, the ratio $(N/Z)_{\text{peak}}$ corresponding to the maximum can be calculated with good precision. In the present case, attempts to use quasi-Gaussian functions or Gram-Charlier series²⁶ have failed. The number of cross sections available to define the parameters of that type of fit was too small, even when taking into account the values published for the same mass interval

TABLE II. Calculated slopes of the linear fits between spallation ratios and (N/Z) ratios of the targets. These results (more detailed in Figs. 7 and 8) show a target "memory effect" in the spallation of medium weight elements.

E_p (GeV)	$38/36\text{Ar}$	$38/39\text{Ar}$	$38/42\text{Ar}$	$22/24\text{Na}$	$42/43\text{K}$
0.15	99 ± 38	-13.9 ± 3.2			
0.3					-31 ± 8
0.4				-4.8 ± 0.5	
0.6					-33 ± 5
1.05	49 ± 4	-6.8 ± 0.3	-2490 ± 265		
24	52 ± 6	-6.9 ± 0.6	-1739 ± 232		

TABLE III. Maxima of the cd curves $\langle N/Z_{\text{peak}} \rangle$ in the mass interval $A=36$ to 42 for targets having different $\langle N/Z \rangle_T$ ratios (see also Figs. 9 and 10). These maxima have been calculated by using a Gaussian fitting function. n is the number of cross sections available for each target in the 24–30 GeV energy region.

Target	Sc	Ti	V	Fe	Co	Ni	Cu
$\langle N/Z \rangle_T$	1.143	1.179	1.217	1.150	1.185	1.100	1.194
$\langle N/Z \rangle_{\text{peak}}$	1.112 ± 0.010	1.116 ± 0.006	1.132 ± 0.005	1.112 ± 0.006	1.114 ± 0.010	1.099 ± 0.007	1.121 ± 0.007
n	4	5	12	7	5	6	10

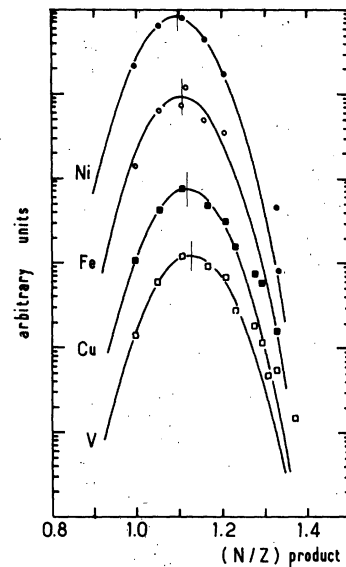


FIG. 9. Charge-dispersion curves in the range $36 \leq A \leq 42$ for Ni, Fe, Cu, and V targets bombarded with 24 GeV protons. Solid curves are Gaussian fits. Vertical lines indicate the calculated maxima of the distributions.

for ^{36}Cl , $^{38,39}\text{Cl}$, $^{37,41}\text{Ar}$, and $^{38,42}\text{K}$ (Refs. 4, 6, 10, 16, 25, and 30). The maxima of the distributions in the 24–30 GeV energy region have therefore been calculated using a Gaussian fit and may be found in Table III and Figs. 9 and 10. Depending on the targets, 4 to 12 cross sections have been used to calculate the three parameters of the function

$$\sigma = a_1 \exp\{-0.5[(x - a_2)/a_3]^2\},$$

in which $a_2 = \langle N/Z \rangle_{\text{peak}}$. It may be noted that the summits of the curves (Fig. 9) are well repre-

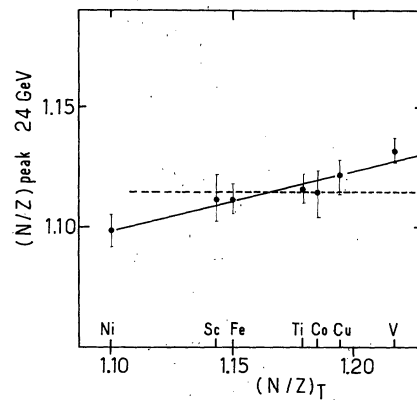


FIG. 10. Peaks of the charge-dispersion curves versus $\langle N/Z \rangle_T$. The solid curve is the best linear fit. The dashed line is the mean of peak values.

sented by a Gaussian function. $(N/Z)_{\text{peak}}$, the ratio at the maximum of the distribution, is calculated with a precision of about 1%. Its value changes by only 3% (1.099 to 1.132) on passing from Ni to V, i.e., from one extreme to the other of the ratios $(N/Z)_T$. The values of $(N/Z)_{\text{peak}}$ are shown in Fig. 10 as a function of $(N/Z)_T$. A linear correlation appears to exist and is given by the equation

$$(N/Z)_{\text{peak}} = (0.831 \pm 0.044) + (0.243 \pm 0.038)(N/Z)_T \dots \quad (2)$$

It may be noted that the mean value of $(N/Z)_{\text{peak}}$ could be considered satisfactory for Sc, Fe, Ti, Co, and even Cu, within the limits of the error bars, but not for Ni and V.

In this charge-dispersion analysis, no correction has been applied for the variation of the mass yield in the $A = 36$ – 42 mass range, since the experimental data required to calculate the nuclear thermometer p were not available for all targets studied here. This approximation is valid for the purpose of calculating the maxima of the cd curves in a narrow range of mass-products when the incident energy is several GeV. The maxima were best determined from data for $A = 38$ and $A = 39$. The results were not significantly changed by assuming a p -value of a few percent per mass unit.

The values of $(N/Z)_{\text{peak}}$ calculated here may be compared, for the same mass region, with those obtained by Husain *et al.*¹⁶ for vanadium (1.130) and by Cumming *et al.*⁶ for copper (1.119 at mass 39). The agreement with these authors is excellent, although the fitting function used by Cumming *et al.* was not the same as that employed here. Ku and Karol, moreover (see Fig. 6 of Ref. 26), obtained a linear correlation between $(N/Z)_{\text{peak}}$ and $(N/Z)_T$ for the spallation of Mo targets. The slope, not calculated by the authors, would appear to be practically the same as that given by Eq. (1) above.

C. Comparison with semiempirical formulas

Only the formula of Silberberg and Tsao²⁴ will be considered here, since it is found to hold over the widest range and is at present the formula most extensively applied to spallation reactions.

The cross sections for Ar isotopes, calculated by means of the Silberberg and Tsao (ST) equation, are shown in Table IV, along with the ratios of calculated to experimental cross sections. These ratios show that disagreement between calculation and experiment is particularly evident in three cases. For $E_p = 150$ MeV, the ratio is greater than 5 for 11 measurements out of 17. Overestimation by the ST formula is systematic at low energies, particularly when the cross sections are

small. When the Ar is produced by peripheral reactions in Sc, the cross sections are again overestimated and, finally, the ST cross sections for $^{36,38,39}\text{Ar}$ and $E_p = 24$ GeV in Ti, V, Fe, Co, Ni, and Cu are too high by at least 30% (the average being 57%, with a distribution of $\pm 27\%$). The ratio for ^{42}Ar at 24 GeV may be greater or less than unity, depending on the target. At $E_p = 0.6$ and 1.05 GeV, the agreement between ST and experiment is excellent for ^{38}Ar and ^{39}Ar and less satisfactory for ^{36}Ar and ^{42}Ar . In particular, the ratio of ST to experimental cross section is greater than six for ^{36}Ar produced in Fe at 600 MeV.

The precision of a semiempirical formula depends on the number and precision of the available cross sections employed to calculate the parameters for a given range of targets, products, and incident energies. In the region defined by $21 \leq Z_T \leq 29$, $36 \leq A \leq 42$, and $0.15 \leq E_p \leq 24$ GeV, the present study provides a greater number of cross sections than were formerly available. These show up discrepancies between the ST and experimental cross sections which were not heretofore evident. In particular, the ST formula does not lead to a maximum in the excitation function and predicts that the latter become constant for energies greater than $E_0 = 69 A_T^{0.867}$. According to the present results, that energy corresponds, rather, to the maximum of the excitation function. The uncertainty of the monitor cross sections alone cannot explain this discrepancy. In addition, although the memory effect concerning the ratio $(N/Z)_T$ is predicted by the ST formula, the predicted influence is too small, especially for isotopes such as ^{42}Ar which are far from stability.

D. Astrophysical implications

An important application of the spallation of medium mass targets is the calculation of the propagation of cosmic rays in the interstellar medium for the elements of the iron peak. The mean energy of the galactic cosmic radiation (GCR) is 3 to 4 GeV/nucleon. The greater part of the hundreds of cross sections necessary for the calculation of GCR propagation is estimated by means of the ST formula. The results of the propagation calculation are very sensitive to the values of the cross sections, so that the ST formula may be expected to give satisfactory results for $E_p = 3$ to 4 GeV and medium-mass targets. For such energies, the calculated excitation functions (ST) are already indistinguishable from the asymptote, whereas the experimental values are in the neighborhood of the maximum. Fortunately, for many reactions studied here, the experimental maximum appears to coincide with the ST asymptote, so that the calculated cross sections are

TABLE IV. Cross sections for Ar isotopes calculated by means of the Silberberg and Tsao equation and ratios of calculated to experimental cross sections. The best agreement between ST and experiment is found for high energy (GeV) incident protons and for products near stability.

Target	E_p (GeV)	0.150 GeV		0.600 GeV		1.05 GeV		24 GeV	
		Calc.	Calc./Expt.	Calc.	Calc./Expt.	Calc.	Calc./Expt.	Calc.	Calc./Expt.
Sc	36	3.18	1.12			3.8	1.30	3.5	2.00
	38	59.9	2.10			46.3	1.67	39.6	2.39
	39	36.9	3.02			23.0	1.68	18.9	2.17
	42	1.23	36.2			0.32	2.91	0.22	2.44
Ti	36	1.29	1.12			2.93	0.86	2.94	1.52
	38	24.2	1.70			35.6	1.16	33.0	1.82
	39	14.9	1.96			17.7	1.05	15.7	1.51
	42	0.50	5.26			0.31	0.63	0.24	0.63
V	36							2.5	1.84
	38							27.9	1.77
	39							13.3	1.29
	42							0.20	0.37
Fe	36	0.12		0.92	6.17	1.6	0.64	2.1	1.53
	38	2.19	6.44	11.6	0.94	18.0	0.99	21.9	2.23
	39	1.27	7.06	5.7	0.93	8.4	0.93	9.8	1.96
	42	0.04		0.11	2.2	0.14	1.27	0.14	1.67
Co	36	0.05	14.3			1.13	0.63	1.7	1.31
	38	0.87	15.0			13.7	0.81	18.8	1.61
	39	0.54	12.9			6.8	0.72	8.9	1.37
	42	0.02	100.0			0.12	0.60	0.13	0.59
Ni	36	0.08	5.7			1.84	0.71	2.78	1.33
	38	0.86	10.8			13.5	0.96	18.6	1.75
	39	0.36	12.4			4.6	0.77	6.0	1.33
	42	0.008				0.05	1.04	0.06	1.30
Cu	36	0.01		0.30	0.79	0.73	0.73	1.38	1.30
	38	0.19		4.0	0.93	9.1	0.91	15.5	1.63
	39	0.12		2.1	0.81	4.4	0.77	7.0	1.30
	42	0.004		0.041	0.72	0.076	0.54	0.11	0.73

probably free of systematic error in the energy region of interest. However, precise excitation functions are needed in order to account for the variation of GCR composition with energy.

The study of rare gases in lunar rocks and meteorites provides considerable information on the history of the solar system. The argon in these extraterrestrial objects arises largely from spallation reactions induced by cosmic radiation. An interesting conclusion of the present work is that the spallation ratios for Ar are almost independent of E_p at high energies: For twelve values of R , the ratios 38/36 and 38/39 at 1 and 24 GeV, we find $R(1)/R(24) = 1.03 \pm 0.04$. This conclusion may be extended to $E_p = 0.6$ GeV for the two targets considered here (Fe and Cu). At lower energies, however, and particularly for reactions corresponding to a small ΔA , these spallation ratios vary appreciably. That effect can become important if samples from deep within the meteorite or below planetary surfaces are considered. Therefore,

the constant production ratios currently being used for Ar isotopes when calculating exposure ages of meteorites are to be examined more carefully.³⁹

ACKNOWLEDGMENTS

I wish to acknowledge the cooperation of the operating staff of the Louvain-la-Neuve, Orsay, Saturne and CERN accelerators. The rare gas analyses were performed with the aid of F. Brout, C. Chouard, M. F. Heland, M. Lagarde-Simonoff, and H. Sauvageon. Special thanks are due to O. Eugster and J. Geiss for their hospitality and their advice on the mass spectrometry method to M. Casse, P. Goret, J. P. Meyer, and H. Reeves for stimulating discussions, and to A. Mackenzie Peers for the English text. I am indebted to G. Simonoff for advice and support during the entire project. Part of this work was supported by DGRST (Contract No. 74-7-0931).

- ¹R. L. Brodzinski, L. A. Ranticelli, J. A. Cooper, and N. A. Wogman, *Phys. Rev. C* **4**, 1250 (1971).
- ²R. L. Brodzinski, L. A. Ranticelli, J. A. Cooper, and N. A. Wogman, *Phys. Rev. C* **4**, 1257 (1971).
- ³M. Lagarde-Simonoff, S. Regnier, H. Sauvageon, G. N. Simonoff, and F. Brout, *J. Inorg. Nucl. Chem.* **37**, 627 (1975).
- ⁴K. F. Chackett, *J. Inorg. Nucl. Chem.* **27**, 2493 (1965).
- ⁵J. B. Cumming, P. E. Haustein, R. W. Stoenner, I. Mausner, and R. A. Naumann, *Phys. Rev. C* **10**, 739 (1974).
- ⁶J. B. Cumming, R. W. Stoenner, and P. E. Haustein, *Phys. Rev. C* **14**, 1554 (1976).
- ⁷J. Hudis, I. Dostrovsky, G. Friedlander, J. R. Grover, N. T. Porile, L. P. Remsberg, R. W. Stoenner, and S. Tanaka, *Phys. Rev.* **129**, 434 (1963).
- ⁸C. J. Orth, H. A. O'Brien, M. E. Schillaci, B. J. Dropesky, J. E. Cline, E. B. Nieschmidt, and R. L. Brodzinski, *J. Inorg. Nucl. Chem.* **38**, 13 (1976).
- ⁹S. Regnier, M. Lagarde, G. N. Simonoff, and Y. Yokoyama, *Earth Planet. Sci. Lett.* **18**, 9 (1973).
- ¹⁰S. Regnier, M. Baklouti, M. Simonoff-Lagarde, and G. N. Simonoff, *Phys. Lett.* **B68**, 202 (1977).
- ¹¹E. Brunix, CERN Report No. 64-17, 1964 (unpublished).
- ¹²R. Silberberg and C. H. Tsao, NRL Report No. 7593, 1973 (unpublished).
- ¹³J. Toballem and C. H. de Lassus St. Geniès, Report No. CEA-N-1466 (3), 1975 (unpublished).
- ¹⁴O. A. Schaeffer and J. Zahringer, *Phys. Rev.* **113**, 674 (1959).
- ¹⁵J. Hudis, T. Kirsten, R. W. Stoenner, and A. O. Schaeffer, *Phys. Rev. C* **1**, 2019 (1970).
- ¹⁶L. Husain and S. Katcoff, *Phys. Rev. C* **7**, 2452 (1973).
- ¹⁷C. Perron, *Phys. Rev. C* **14**, 1108 (1976).
- ¹⁸R. Serber, *Phys. Rev.* **72**, 1008 (1947).
- ¹⁹G. Rudstam, *Philos. Mag.* **44**, 1131 (1953).
- ²⁰G. Rudstam, *Z. Naturforsch.* **21a**, 1027 (1966).
- ²¹H. Reeves, *Annu. Rev. Astron. Astrophys.* **12**, 437 (1974).
- ²²M. M. Shapiro and R. Silberberg, *Philos. Trans. R. Soc. London* **A277**, 319 (1975).
- ²³R. C. Reedy and J. R. Arnold, *J. Geophys. Res.* **77**, 537 (1972).
- ²⁴R. Silberberg and C. H. Tsao, *Astrophys. J. Suppl. Ser.* **220**, 25, 315 (1973).
- ²⁵N. T. Porile and L. B. Church, *Phys. Rev.* **133**, B310 (1964).
- ²⁶T. H. Ku and P. J. Karol, *Phys. Rev. C* **16**, 1984 (1977).
- ²⁷J. Toballem, C. H. de Lassus St. Genies, and L. Leveque, Report No. CEA-N-1466 (1), 1971 (unpublished).
- ²⁸S. Regnier, Ph. D. thesis, Bordeaux, 1977 (unpublished).
- ²⁹K. Goebel, H. Schultes, and J. Zahringer, CERN Report No. 64-12, 1964 (unpublished).
- ³⁰M. A. Forman, R. W. Stoenner, and R. Davis, *J. Geophys. Res.* **76**, 4109 (1971).
- ³¹A. Cheng, Ph.D. thesis, Stony Brook, 1972 (unpublished).
- ³²V. S. Barashenkov, A. S. Iljinov, N. M. Sobolevski, and V. D. Toneev, *Usp. Fiz. Nauk.* **109**, 91 (1973) [*Sov. Phys. Usp.* **16**, 31 (1973)].
- ³³M. Lagarde-Simonoff, S. Regnier, H. Sauvageon, and G. N. Simonoff, *Nucl. Phys.* **A260**, 369 (1976).
- ³⁴G. M. Raisbeck and F. Yiou, in *Proceedings of the Fourteenth International Conference on Cosmic Rays, 1975, Munich*, edited by Klaus Pinkau (Max-Planck-Institute, München, 1975).
- ³⁵G. M. Raisbeck, F. Yiou, in *Proceedings of the Fifteenth International Conference on Cosmic Rays, Plovdiv, 1977*, Report No. OG 142 (unpublished).
- ³⁶G. English, Y. W. Yu, and N. T. Porile, *Phys. Rev. C* **10**, 2281 (1974).
- ³⁷R. G. Korteling and A. A. Caretto, *J. Inorg. Nucl. Chem.* **29**, 2863 (1967).
- ³⁸R. H. Bieri and W. Rutsch, *Helv. Phys. Acta* **35**, 553 (1962).
- ³⁹K. Marti and S. Regnier, *Meteoritics* **13**, 551 (1978).